

Table S1. Crystal data and structure refinement for **2**, **3**, and **4·2CH₃CN**.

Compound	2	3	4·2CH₃CN
Empirical formula	C ₃₄ H ₅₁ B ₁₂ CdN ₇ O ₃	C ₂₄ H ₃₂ N ₆ O ₄ Zn	C ₂₄ H ₄₆ B ₁₂ N ₈
Formula weight	847.93	533.92	576.41
Temperature/K	100.00	100.00	100.00
Crystal system	triclinic	monoclinic	triclinic
Space group	<i>P</i> -1	<i>P</i> 2 ₁ / <i>n</i>	<i>P</i> -1
a/Å	10.494(2)	13.8012(15)	8.036(2)
b/Å	12.322(4)	12.687(2)	10.416(4)
c/Å	18.644(6)	15.896(2)	10.700(4)
$\alpha/^\circ$	79.582(13)	90	106.211(14)
$\beta/^\circ$	87.114(11)	115.116(5)	91.220(12)
$\gamma/^\circ$	75.755(11)	90	109.216(10)
Volume/Å ³	2298.1(12)	2520.3(7)	805.8(4)
Z	2	4	1
$\rho_{\text{calcg}}/\text{cm}^3$	1.225	1.407	1.188
μ/mm^{-1}	0.515	1.016	0.067
F(000)	872.0	1120.0	306.0
Radiation	MoKα ($\lambda = 0.71073$)	MoKα ($\lambda = 0.71073$)	MoKα ($\lambda = 0.71073$)
Index ranges	-13 ≤ h ≤ 13, -16 ≤ k ≤ 12, -24 ≤ l ≤ 18	-19 ≤ h ≤ 19, -17 ≤ k ≤ 13, -22 ≤ l ≤ 22	-11 ≤ h ≤ 11, -10 ≤ k ≤ 14, -15 ≤ l ≤ 14
Reflections collected	14162	20891	6246
Independent reflections	10200 [$R_{\text{int}} = 0.0263$, $R_{\text{sigma}} = 0.0803$]	7064 [$R_{\text{int}} = 0.0333$, $R_{\text{sigma}} = 0.0422$]	4553 [$R_{\text{int}} = 0.0221$, $R_{\text{sigma}} = 0.0549$]
Data/restraints/parameters	10200/0/520	7064/0/339	4553/0/201
Goodness-of-fit on F^2	1.021	1.028	1.037
Final <i>R</i> indexes [$I \geq 2\sigma(I)$]	$R_1 = 0.0503$, wR ₂ = 0.1050	$R_1 = 0.0336$, wR ₂ = 0.0728	$R_1 = 0.0483$, wR ₂ = 0.1084
Final <i>R</i> indexes [all data]	$R_1 = 0.0727$, wR ₂ = 0.1149	$R_1 = 0.0506$, wR ₂ = 0.0784	$R_1 = 0.0656$, wR ₂ = 0.1171

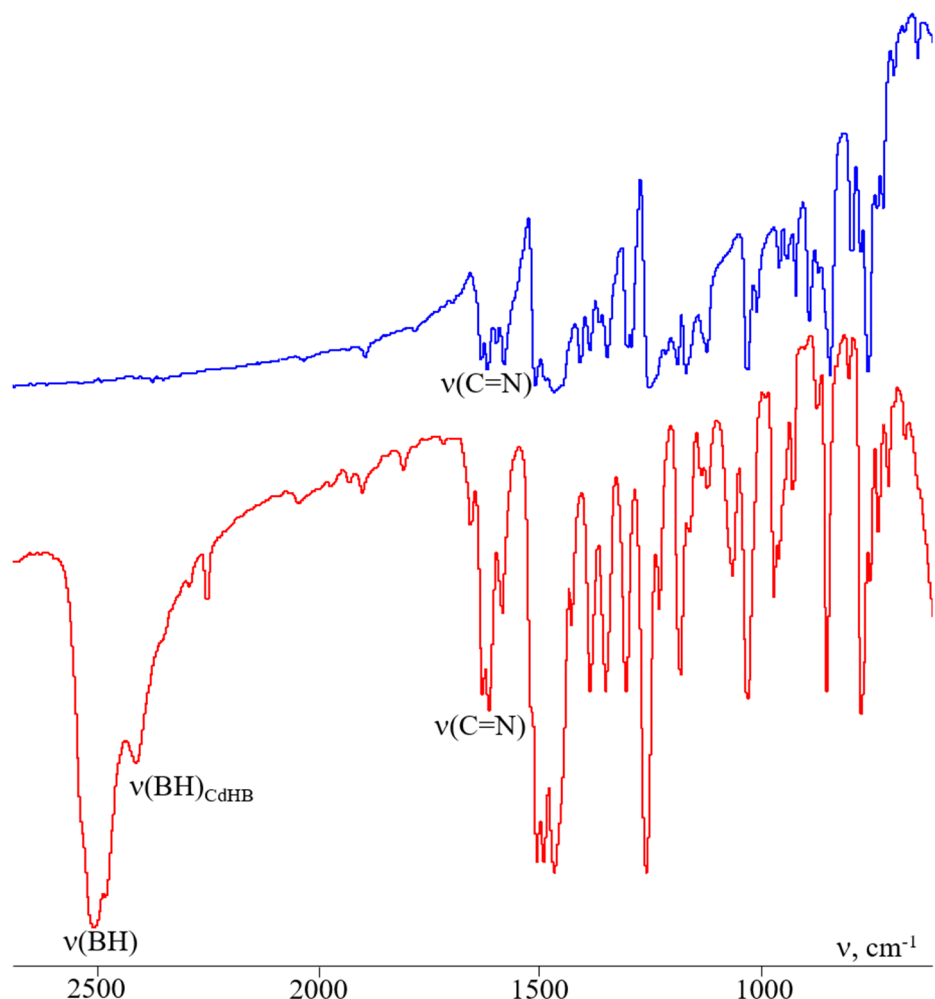


Figure S1. IR spectra of ligand L^1 (blue) and complex **1** (red).

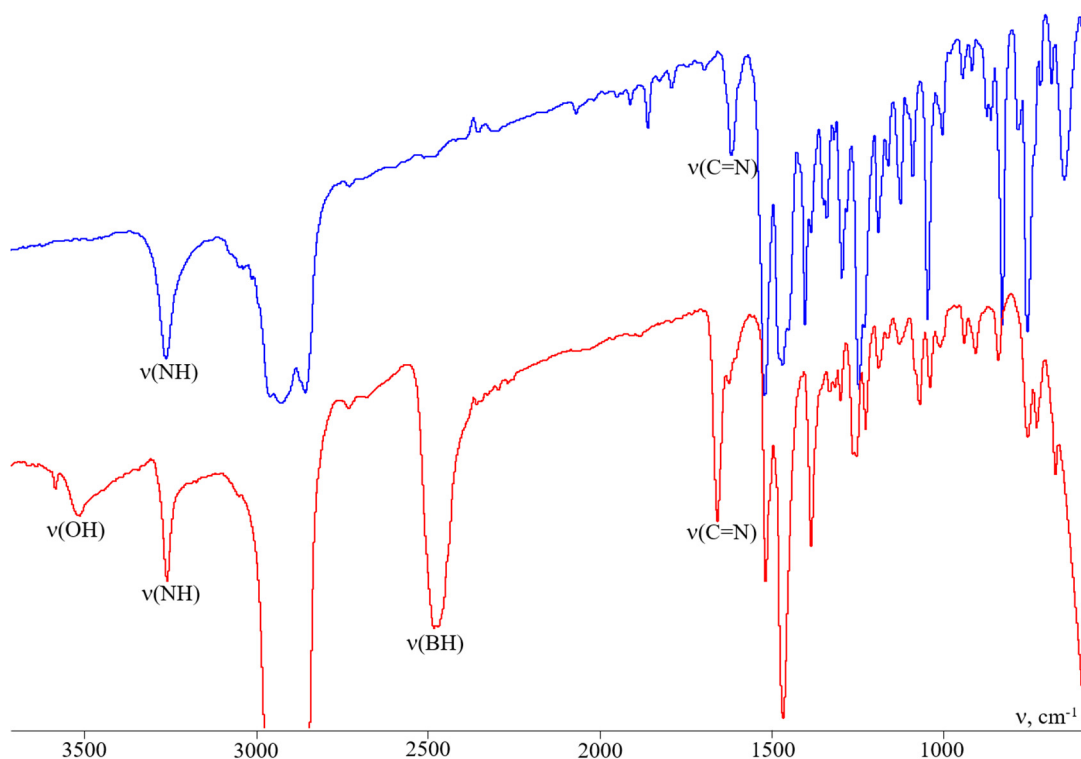


Figure S2. IR spectra of ligand L^2 (blue) and complex **2** (red).

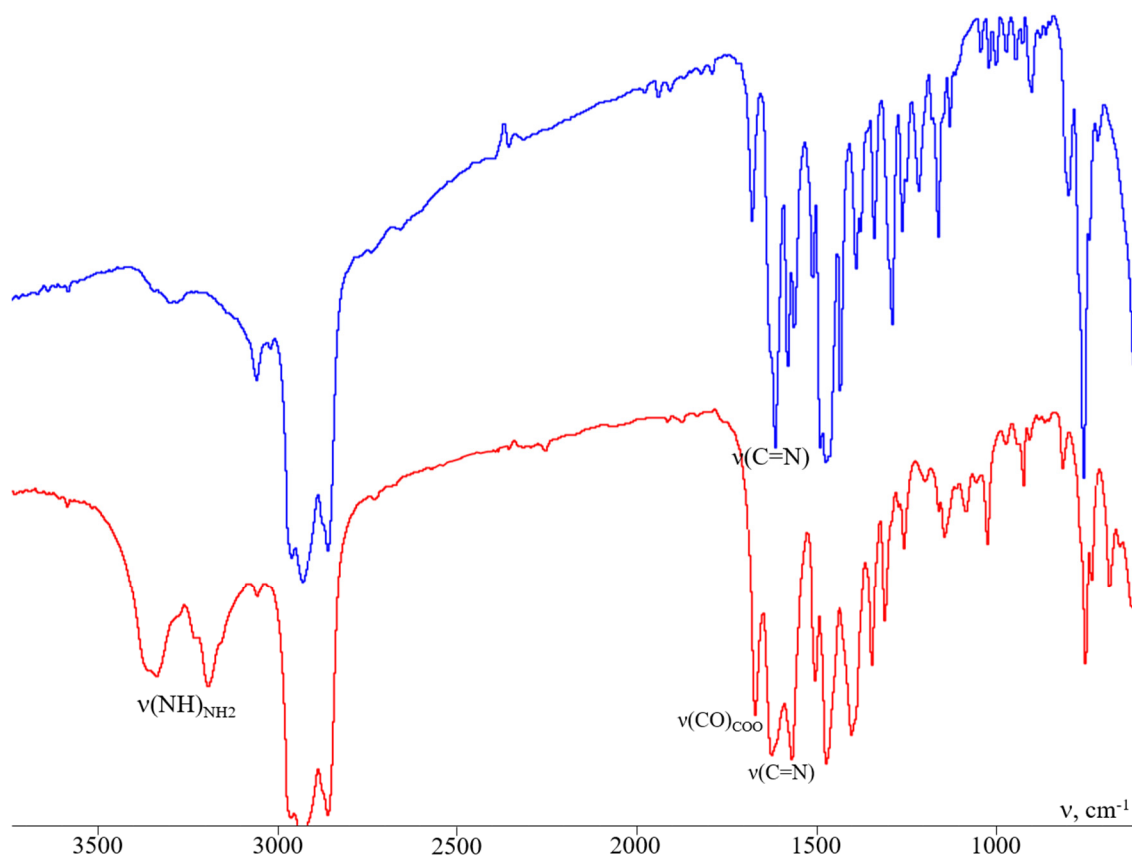


Figure S3. IR spectra of ligand L³ (blue) and complex 3 (red).

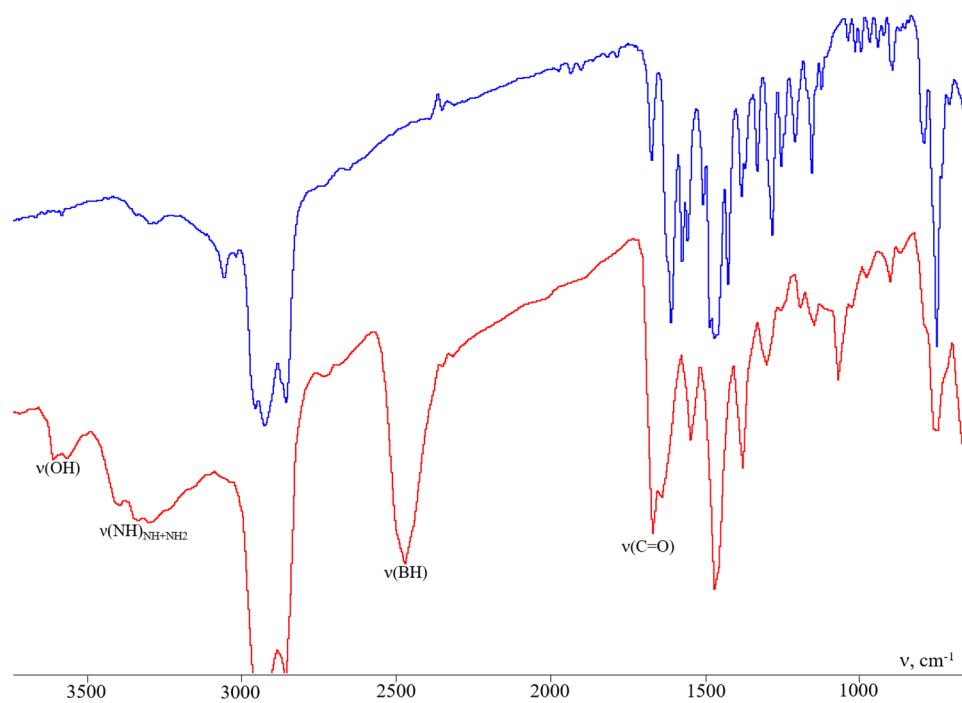


Figure S4. IR spectra of ligand L³ (blue) and a precipitate containing (HBz-NH₂)₂[B₁₂H₁₂] (4) and a cadmium(II) complex with salicylaldehyde (red).

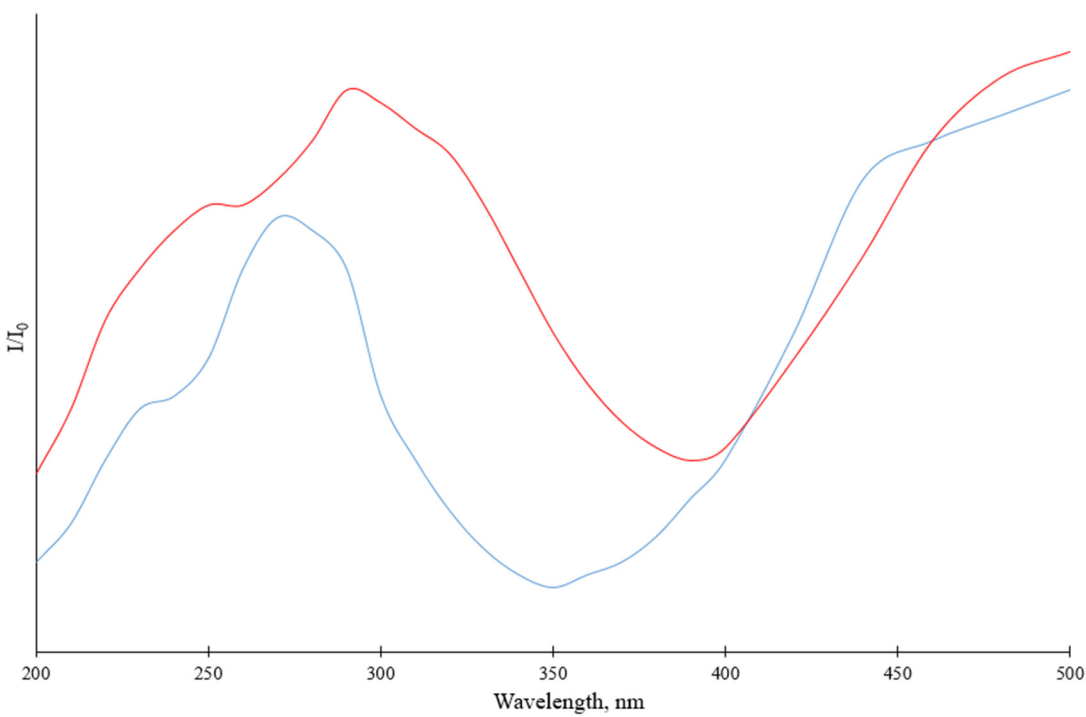


Figure S5. UV-vis absorption spectra of ligand L^1 (blue) and complex $\mathbf{1}$ (red).

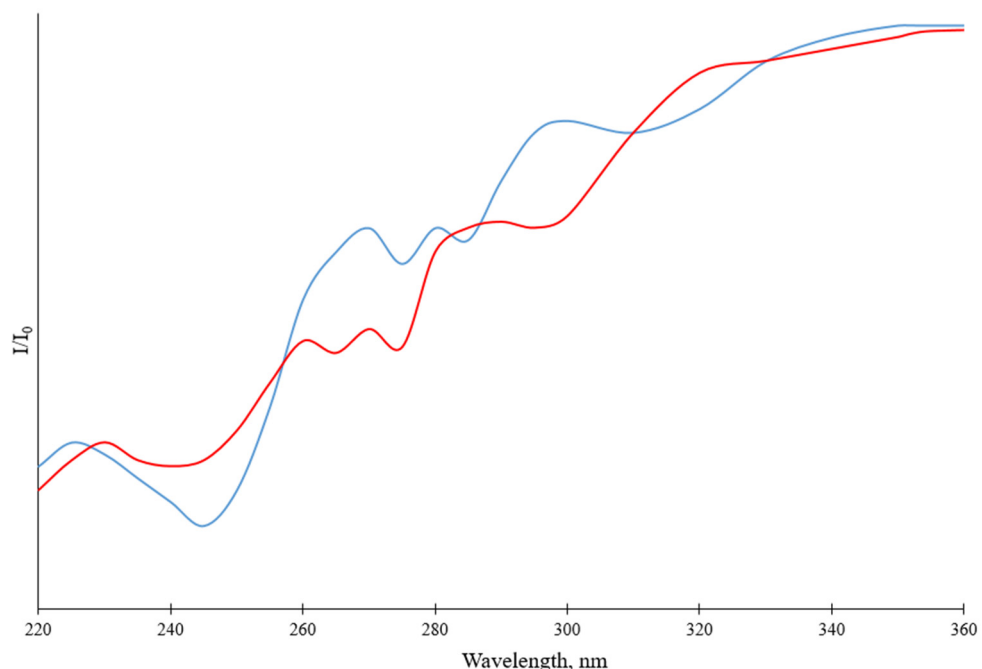


Figure S6. UV-vis absorption spectra of ligand L^2 (blue) and complex $\mathbf{2}$ (red).

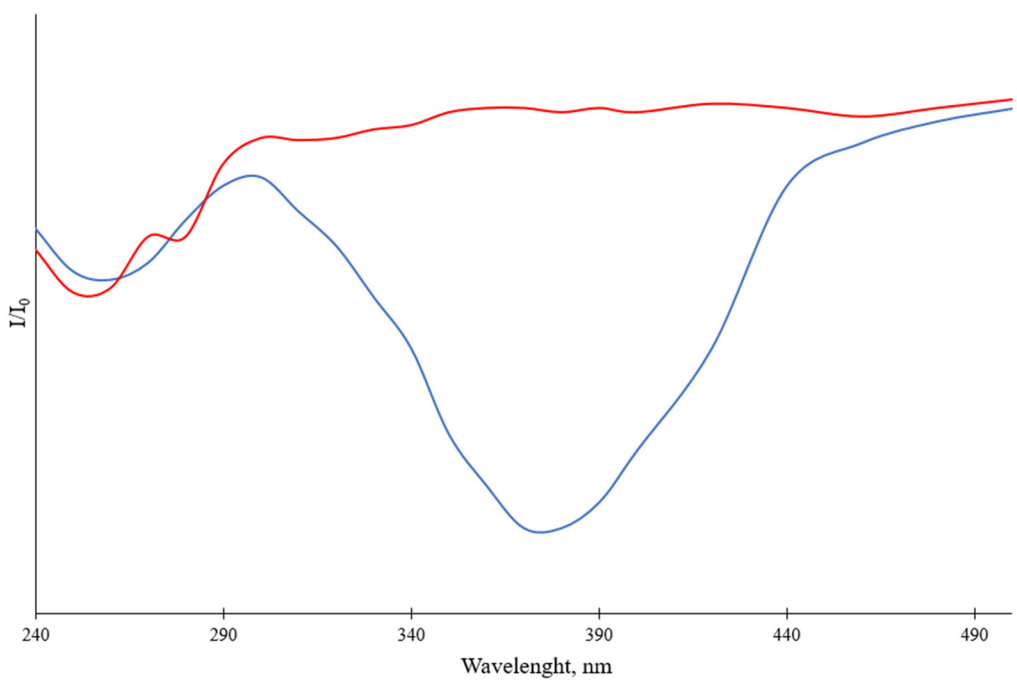


Figure S7. UV-vis absorption spectra of ligand L^3 (blue) and complex **3** (red).

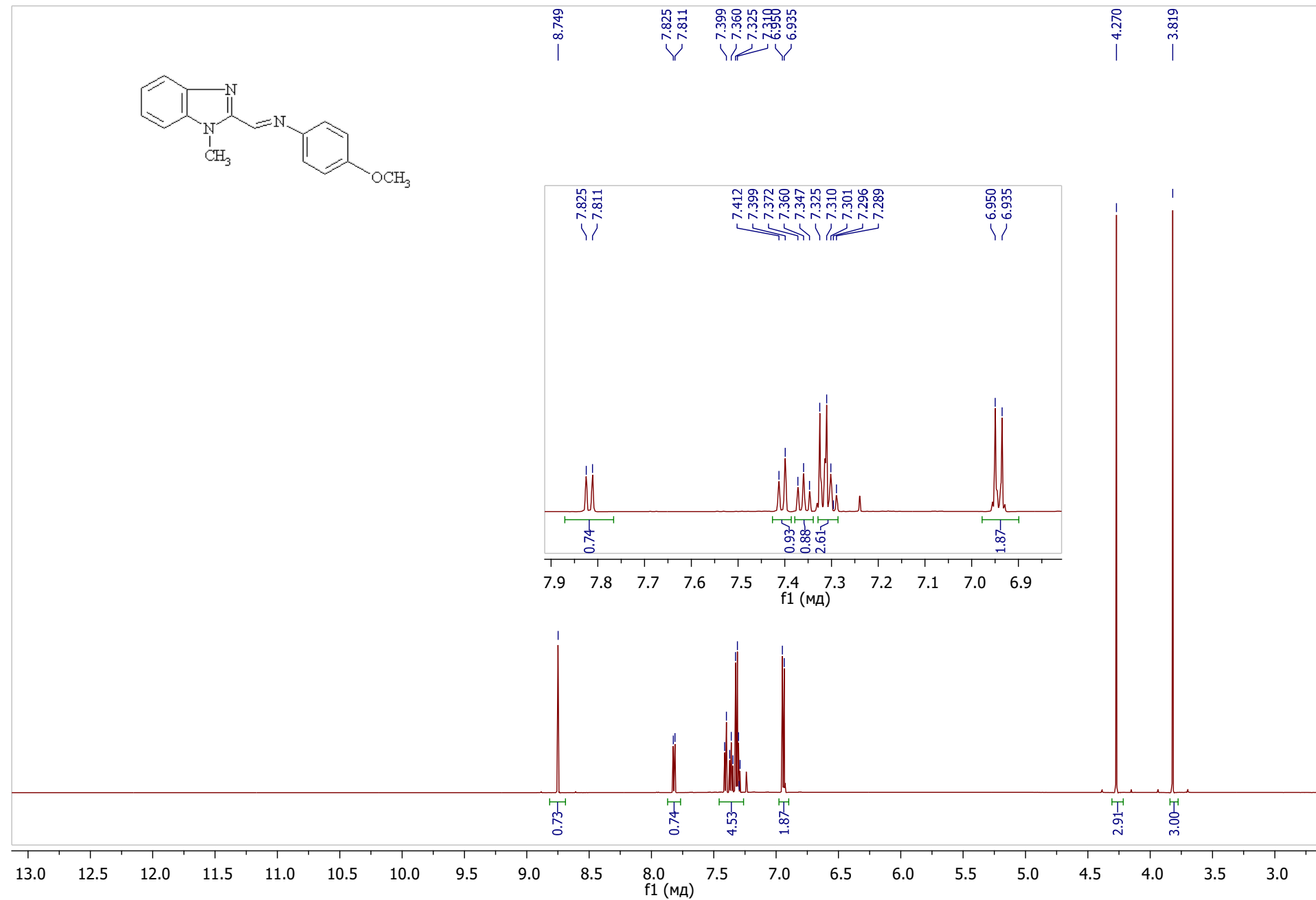


Figure S8. ^1H NMR spectrum of N -(4-methoxyphenyl)-1-(1-methylbenzimidazol-2-yl)methanimine (L^1).

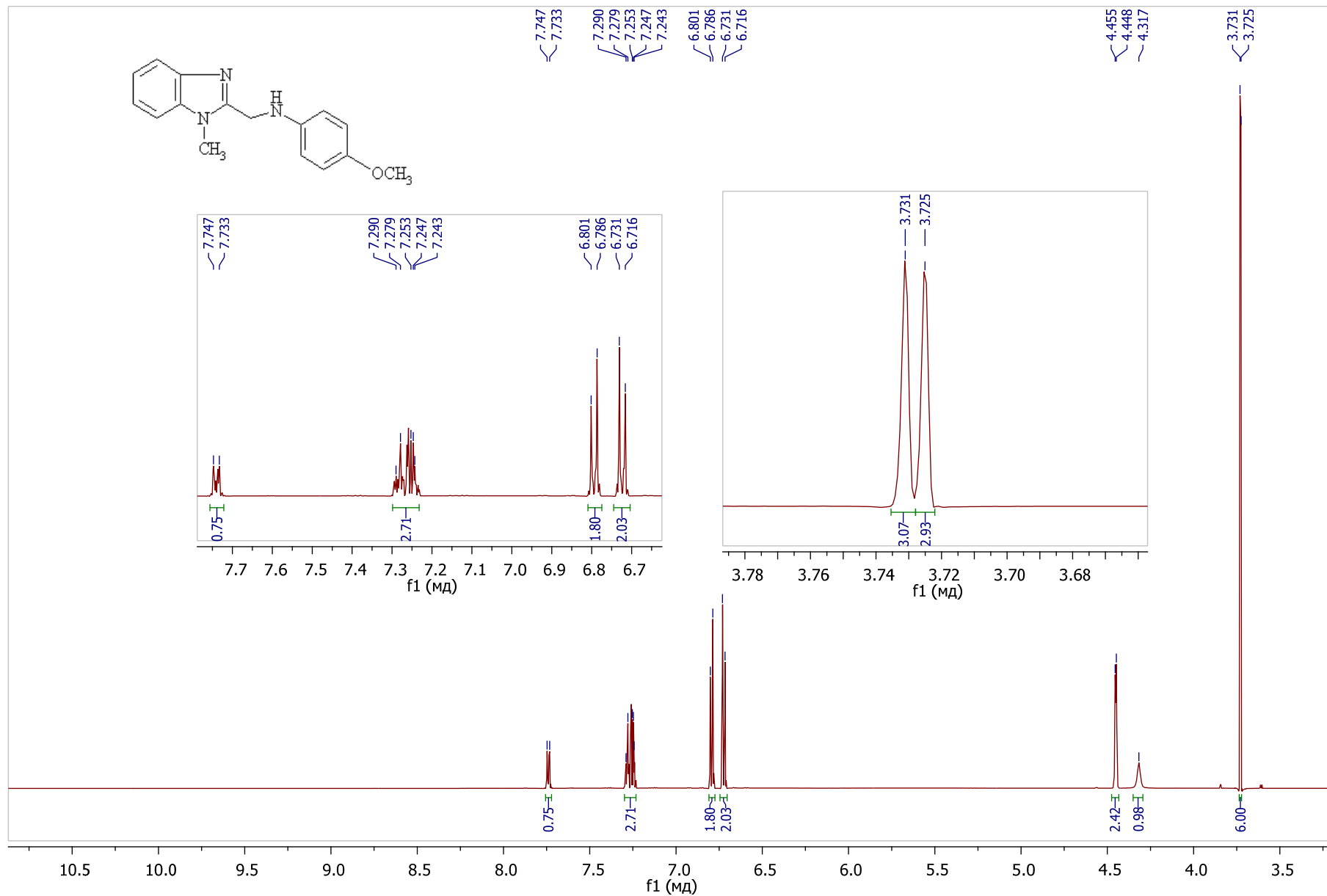


Figure S9. ^1H NMR spectrum of 4-methoxy- N -[(1-methylbenzimidazol-2-yl)methyl]aniline (L^2).

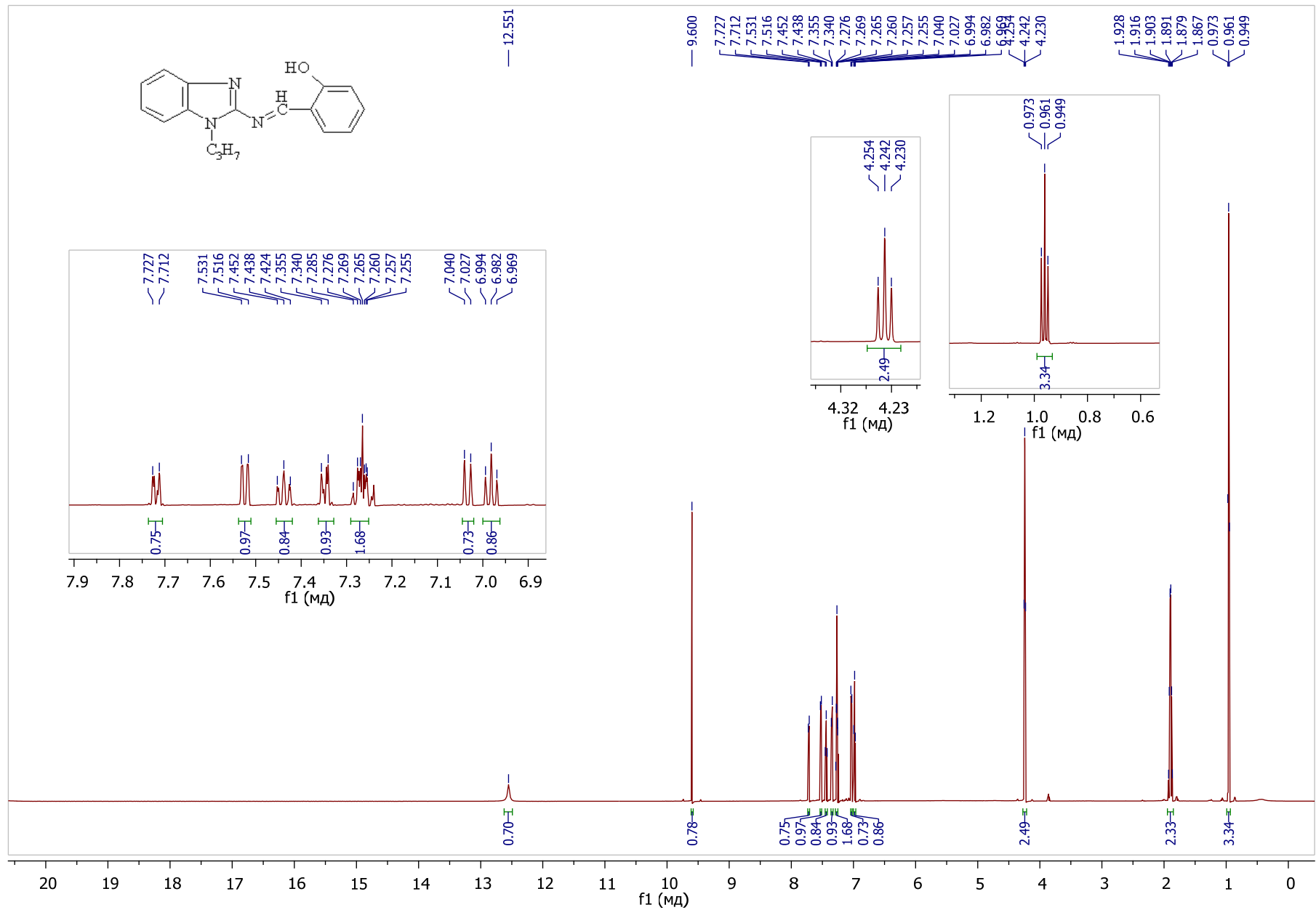


Figure S10. ^1H NMR spectrum of 2-[*(E*)-(1-propylbenzimidazol-2-yl)iminomethyl]phenol (L^3).

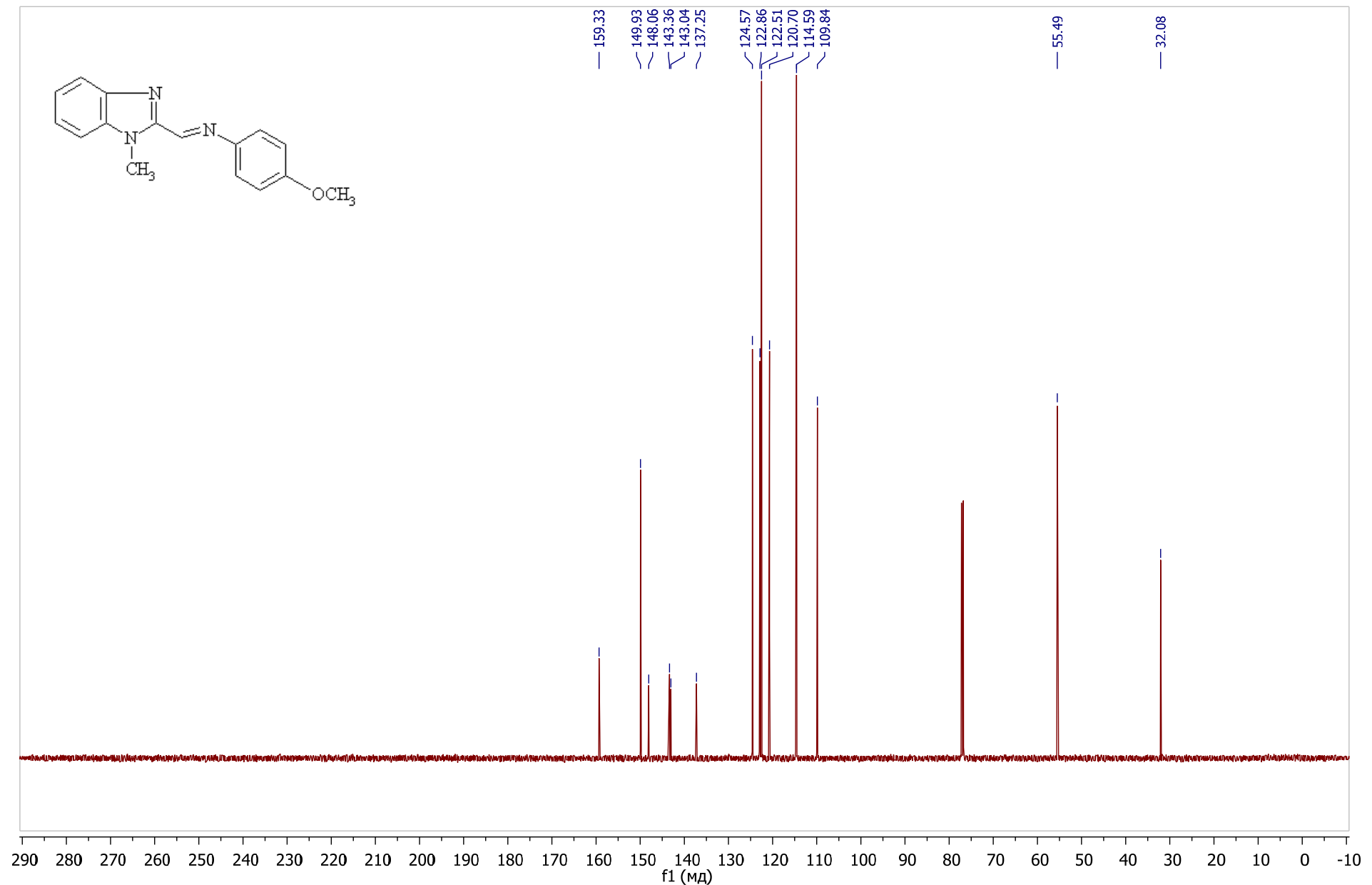


Figure S11. ^{13}C NMR spectrum of $\text{N}-(4\text{-methoxyphenyl})\text{-1-(1-methylbenzimidazol-2-yl)methanimine}$ (L^1).

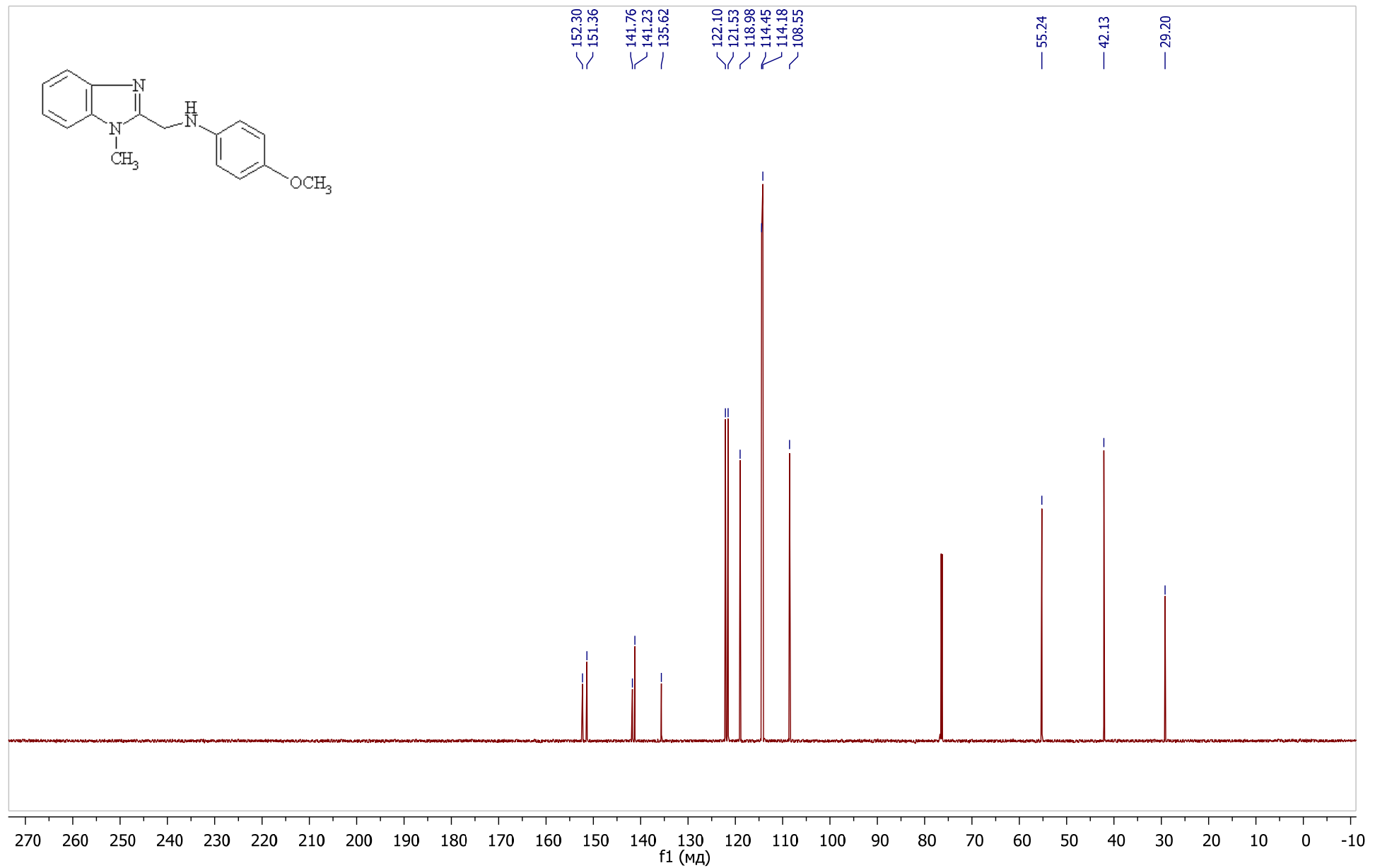


Figure S12. ^{13}C NMR spectrum of 4-methoxy-*N*-[(1-methylbenzimidazol-2-yl)methyl]aniline (L^2).

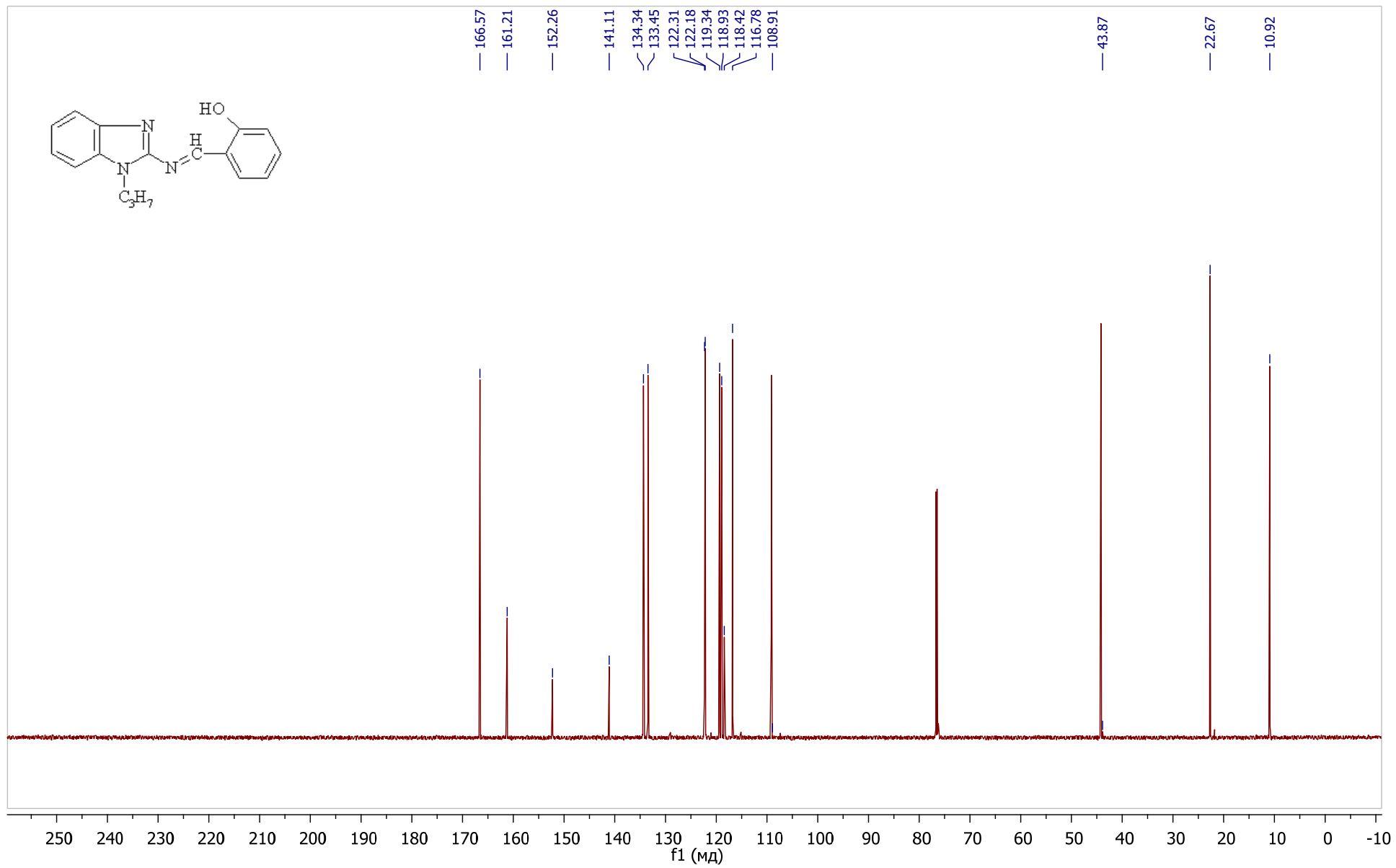


Figure S13. ^{13}C NMR spectrum of 2-[{(E)-(1-propylbenzimidazol-2-yl)iminomethyl}phenol (L^3).

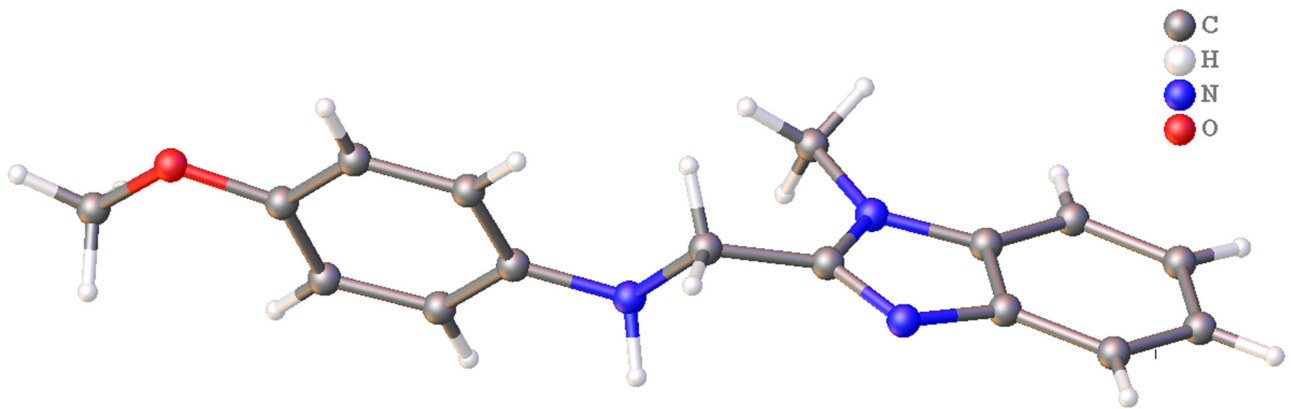


Figure S14. Structure of ligand L^2 .